

U. S. DEPARTMENT OF COMMERCE
NATIONAL OCEANIC AND ATMOSPHERIC ADMINISTRATION
NATIONAL WEATHER SERVICE
NATIONAL METEOROLOGICAL CENTER

OFFICE NOTE 75

A Description of the NMC Planetary Boundary Layer Model

E. Gross, R. Jones, R. McPherson
Development Division

JUNE 1972

1. Introduction

The Planetary Boundary Layer (PBL) modeling project has been underway at the National Meteorological Center since September 1971. It was originally conceived as an effort to adapt an existing model designed by Gerrity (1967) under an Air Force contract, and implemented in modified form at the Air Force Global Weather Central in March 1969 (Hadeen, 1970) to function in the NMC environment. The intent was to then test the utility of the model and the feasibility of its routine operation at NMC. The first stage of this task is now complete; the PBL model does function at NMC and has been run on several cases.

The project has rather naturally divided itself into three main areas: the construction of an objective analysis model, the prediction model itself, and the output package. This office note draws together three sets of notes, each describing one of these areas, in a first attempt to document our work on the PBL project. Each set is quite lengthy and detailed, in a deliberate effort to set forth how the complete package actually works. The intended readership, then, is not the casual reader with only a passing interest in boundary layer modeling, but rather he who is interested in the functioning of the model. Undoubtedly, such persons are very scarce and their ranks may be even thinner after encountering this note.

It is presumed that the reader is familiar with Gerrity's original paper. No attempt is made here to present the physical basis of the model, or its mathematical derivation; both are available in Gerrity's paper.

2. Prognostic Model

This section will describe the form and operation of the prognostic PBL model as it currently functions in the NMC environment. It is our intent to describe the manner in which the PBL code actually operates, and to draw attention to both the attractive aspects of, and the warts on, its image.

The approach taken here will be to follow the logic of the computational sequence; each subroutine of the computer code will be discussed in the sequence it is called by the main program. As this is done, the computations will be related to the model equations, and each such equation will be designated by its number in Gerrity's paper, in parentheses. We will occasionally take note of AFGWC modifications to Gerrity's original formulation, and modifications made at NMC will be noted, but the primary purpose of this section is an exposition of how the PBL model works, rather than an analysis of the various modifications that have been made.

The integrations are carried out on a grid lattice of 29 x 27 regular points separated by a constant increment on a polar stereographic projection of the Northern Hemisphere. The separation between grid points is equal to 190.5 km at 60°N. The grid lattice is a subset of the Limited-area Fine Mesh (LFM) model grid, as shown in Figure 1.

In the vertical, seven levels of information are carried from the surface to 1600 meters above the surface. The vertical coordinate follows the terrain as is illustrated in Figure 2.

The first task is to provide the model with the initial fields of temperature and specific humidity, and also certain fixed fields, such as elevation, roughness length, latitude and longitude, and the radiation coefficients.¹ The latter are climatologically-determined amplitudes of the diurnal temperature wave. Boundary conditions at the 1600 m level are also required. The LFM model provides the values of u- and v-components of the wind, interpolated to 1600 m AGL from the available tropospheric wind components. In addition, an estimate of free air cloudiness is required. This estimate has been inferred from the mean relative humidity in the tropospheric layers of the LFM, based upon the following arbitrary classification:

Mean RH	DCLD
0-50	1
51-80	2
>80	3

Once the initial data and boundary conditions have been made available to the model, control then shifts to the actual computational sequences of the marching process. The first procedure is the adjustment of the surface specific humidity due to moisture sources.²

The necessary parameters are the "percent wetted area," M, the surface temperature, and the elevation. The "percent wetted area" is calculated according to

$$M = (q_h - q_i) / (q_h - q_{is}) \quad (G2.87) \quad (1)$$

where h refers to the top of the contact layer (50 m), i refers to instrument shelter level, and s denotes a saturation value. This calculation is done in the analysis package, and is transmitted to the forecast model as a fixed field. Surface saturation specific humidity q_{is} is next calculated, using Tetten's formula

$$q_s = \frac{3.8 \times 10^{-3}}{[1.013 - 1.065 \times 10^{-6} (z+E)]} \exp \left[17.25 \left(\frac{T-273.0}{T-35.7} \right) \right] \quad (G2.31) \quad (2)$$

¹Accomplished by a call from the main program to subroutine DATAIN.

²Subroutine GRNDWT.

where z for the instrument shelter level is 122 cm, E is elevation, and T is temperature. Then using the value M and the 50 m specific humidity q_h , the surface specific humidity is calculated from

$$q_i(t) = M q_{is}(t) + (1-M) q_h(t), \quad (G2.88) \quad (3)$$

and the result is stored.³ It is important to note that this procedure results in a modification only to the initial analysis of surface specific humidity. Throughout the entire forecast, evaporation from surface sources is not allowed. This result was not intentional but arises from a programming error, which was not discovered until recently.

The remaining computational subroutines are employed at each time step. The first in the sequence⁴ computes the formulae for the geostrophic wind components at each level, as well as the quantities \tilde{u} and \tilde{v} , which are a sort of geostrophic wind component due to the slope of the terrain.

This is first accomplished by calculating over the entire grid,

$$A_{\ell,m} = \frac{1}{2} \left(\frac{1}{H-h} \right) \sum_{k=2}^7 \Delta z_k \left(\frac{1}{T_{\ell,m,k}} + \frac{1}{T_{\ell,m,k-1}} \right), \quad (4)$$

where $H = 1600$ m, and Δz_k is the vertical spacing between layers. Then, corresponding to \tilde{u} , over all points except the boundary,

$$DU_{\ell-m} = \frac{mg}{f} \left(\frac{E_{\ell,m-1} - E_{\ell,m+1}}{2\Delta x} \right) \quad (G2.28) \quad (5)$$

where m is the map factor, and f is the Coriolis parameter, and likewise for \tilde{v} ,

$$DV_{\ell,m} = \frac{mg}{f} \left(\frac{E_{\ell+1,m} - E_{\ell-1,m}}{2\Delta x} \right) \quad (G2.29) \quad (6)$$

³In array QHAT

⁴Subroutine PREWIND

The horizontal derivatives of the integral A are then calculated and stored in arrays $B_{\ell,m}$ and $C_{\ell,m}$

$$B_{\ell,m} = \frac{mg}{f} \left(\frac{A_{\ell,m-1} - A_{\ell,m+1}}{2\Delta x} \right) \quad (7)$$

$$C_{\ell,m} = - \frac{mg}{f} \left(\frac{A_{\ell+1,m} - A_{\ell-1,m}}{2\Delta x} \right). \quad (8)$$

Finally, the boundary values of DU, DV, B, and C are set equal to their calculated values of the points immediately adjacent to the boundary.

After these elements have been calculated, they are combined to obtain the geostrophic wind components u_g and v_g .⁵ First, the appropriate geostrophic⁶ wind components at $z \equiv H$ (1600 m) are obtained from the boundary conditions. Since only hourly values of the boundary conditions are available, linear interpolation in time between adjacent hourly values is necessary if the marching process is at a half-hour time.

The geostrophic u-component is calculated over the entire horizontal array and for each of the levels from 50 m to 1600 m,⁷

$$u_g = u_g^H \left[1 + \left(\frac{T_h - T_H}{T_H} \right) \left(\frac{H-z}{H-h} \right) \right] - T_h(H-z)B + \left(\frac{T_h - T_H}{T_H} \right) \left(\frac{H-z}{H-h} \right) DU, \quad (G2.26) (9)$$

The surface geostrophic u-component u_{gs} is then calculated from the above formula with $z = 0$.⁸ Similarly, the geostrophic v-component is calculated,⁹

$$v_g = v_g^H \left[1 + \left(\frac{T_h - T_H}{T_H} \right) \left(\frac{H-z}{H-h} \right) \right] - T_h(H-z)C + \left(\frac{T_h - T_H}{T_H} \right) \left(\frac{H-z}{H-h} \right) DV, \quad (G2.27) (10)$$

⁵Subroutine GWNDAD.

⁶The 1600 m winds are not geostrophic in the NMC version, since they are obtained from a primitive equation model. This represents a difference between the NMC and AFGWC versions, since the latter obtains boundary condition winds from a quasi-geostrophic model.

⁷Stored in array U.

⁸Stored temporarily in array A.

⁹Stored in array V.

and the surface geostrophic v-component v_{gs} is computed again with $z = 0$.¹⁰ The surface geostrophic wind speed is then calculated:¹¹

$$G = (u_{gs}^2 + v_{gs}^2)^{\frac{1}{2}}. \quad (11)$$

The surface geostrophic wind speed is not allowed to become less than 1 m sec^{-1} .

The logarithm (base 10) of the surface Rossby number is then calculated using the equation

$$R_o = \frac{G}{f z_o} \quad (G2.47) \quad (12)$$

where z_o is the roughness length, also transmitted to the model as a fixed field. Then the friction velocity is computed using

$$u_{*N} = G(0.07625 - 0.00625 \log R_o) \quad (G2.48) \quad (13)$$

where the N denotes a value appropriate for neutral stratification.¹² The angle of deviation between the surface geostrophic wind and the wind in the constant flux layer is then calculated:¹³

$$\psi = .625(\log R_o)^2 - 12.75 \log R_o + 80.625. \quad (G2.49) \quad (14)$$

Finally, the ratios of the 50 m u- and v-components to the 50 m wind speed are determined from:

$$C \equiv \frac{u_h}{(u_h^2 + v_h^2)^{\frac{1}{2}}} = \left[\frac{A}{(A^2 + B^2)^{\frac{1}{2}}} \right] \cos(\psi) - \left[\frac{B}{(A^2 + B^2)^{\frac{1}{2}}} \right] \sin(\psi) \quad (15)$$

and

$$RDREX = \frac{v_h}{(u_h^2 + v_h^2)^{\frac{1}{2}}} = \left[\frac{B}{(A^2 + B^2)^{\frac{1}{2}}} \right] \cos(\psi) + \left[\frac{A}{(A^2 + B^2)^{\frac{1}{2}}} \right] \sin(\psi) \quad (16)$$

¹⁰Stored temporarily in array B.

¹¹Stored temporarily in array C.

¹²Stored temporarily in array USTAR.

¹³Stored temporarily in array PHI.

It is next necessary to determine the appropriate convection regime and, based upon that determination, apply the appropriate formulas to calculate the winds, exchange coefficient, and heat flux at the top of the contact layer.¹⁴ These calculations are performed over the entire array.

First, the quantity¹⁵

$$A = \frac{T_h - T_i}{h - z_i} + \frac{g}{c_p} \quad (17)$$

is calculated (subscript i indicates instrument shelter height). If the lapse rate is less than the dry adiabatic, A is positive and the friction velocity u_* is reduced by 20%. If A is negative, lapse conditions prevail, and u_* is augmented by 20%. These adjustments were suggested by Lettau (1959). Next is calculated the quantity¹⁶

$$B = \frac{u_*^2 \overline{\theta}}{4\beta g} \left(\frac{\ln(h/z_i)}{k(h-z_i)} \right)^2 \quad (18)$$

The first test to determine the appropriate convection regime is now performed; if the quantity A-B is negative, control shifts to the free convection formulas. This means that, since $B < 0$ always, A must be negative (i.e., superadiabatic) and larger than B in order that the free convection formulation be used. This is equivalent to allowing the lapse rate to be slightly superadiabatic under forced convection; or stated alternatively, that the forced-convection formulation is valid for small negative Richardson's numbers. If the free convection formulation is selected on the basis of the above test, the expression

$$T_h = T_i - \frac{g}{c_p} (h - z_i) - \frac{3u_* \overline{\theta}}{\lambda^{2/3} |u_* \overline{\theta}|^{1/3}} \left(\frac{\overline{\theta}}{g} \right)^{1/3} \left(h^{-1/3} - z_i^{-1/3} \right) \quad (G2.70) \quad (19)$$

¹⁴Subroutine STRAB

¹⁵This is the left side of Gerrity's inequality (G2.74).

¹⁶This is the right side of Gerrity's inequality (G2.74).

is solved for the cube root of the heat flux $|u_* \theta_*|^{1/3}$. Eqn. (19) arises from the constant-flux formula

$$K \left(\frac{\partial T}{\partial z} + \frac{g}{c_p} \right) = u_* \theta_* \quad (G2.51) \quad (20)$$

integrated between z_i and z_h , with the free-convection definition of the mixing coefficient K ,

$$K = \lambda z^2 \left(\frac{g}{\theta} \left| \frac{\partial T}{\partial z} + \frac{g}{c_p} \right| \right)^{1/2}. \quad (G2.69) \quad (21)$$

The quantity $|u_* \theta_*|^{1/3}$ is then employed to calculate the eddy viscosity K_m at the top of the contact layer from¹⁷

$$K_m = \frac{1}{1.3} \left(\lambda^2 h^4 \frac{g}{\theta} |u_* \theta_*| \right)^{1/3} \quad (G2.73) \quad (22)$$

The next step is to solve

$$S_h = \frac{u_*}{k} \ln \left(\frac{z_o + z_i}{z_o} \right) - \frac{3.9 u_*^2}{\lambda^{2/3} |u_* \theta_*|^{1/3}} \left(\frac{\theta}{g} \right)^{1/3} \left[h^{-1/3} - (z_o + z_i)^{-1/3} \right] \quad (G2.72) \quad (23)$$

for the 50 m wind speed S_h . It is then assumed that a logarithmic wind profile exists below instrument shelter level (122 cm), so that the surface wind speed may be calculated from logarithmic profile law. In view of the fact that observed surface winds are measured at the 10 m level, we have opted to evaluate the surface wind speeds at 10 m. Finally, the quantity $(u_* \theta_*)^{1/3}$ is cubed to obtain the heat flux.

Now, if the test described previously on the quantity (A-B) turns out to be positive, then control shifts tentatively to the forced convection formulation. The equation

$$u_* \theta_* = - \frac{u_*^3 \bar{\theta} \ln(h/z_i)}{2\beta g k(h-z_i)} \left[1 - \left(1 + \frac{4\beta g}{u_*^2 \bar{\theta}} \left(\frac{T_h - T_i}{h - z_i} + \frac{g}{c_p} \right) \left(\frac{k(h-z_i)}{\ln(h/z_i)} \right)^2 \right)^{1/2} \right] \quad (G2.58) \quad (24)$$

¹⁷It should be noted that the exponent of the bracketed quantity in Gerrity's Eqn. (2.73) should be $\frac{1}{3}$ rather than $\frac{2}{3}$.

is used first to calculate the heat flux. Then the quantity

$$\left(1 + \frac{\beta g}{\theta} \frac{u_* \theta_*}{u_*^3} kh\right)^{-1} \quad (25)$$

is calculated, and this is used in

$$K_m = k u_* \left(1 + \frac{\beta g}{\theta} \frac{u_* \theta_*}{u_*^3} kh\right)^{-1} \quad (G2.64) \quad (26)$$

to calculate the eddy exchange coefficient. At this point, the quantity A is tested for positive values.

If A is positive (lapse rate less than the dry adiabatic.....i.e., stable conditions), then the quantity

$$X = \left[\frac{(h-z_i) \bar{\theta}}{\beta g A} u_*^2 \right]^{1/3} \quad (27)$$

is calculated. This quantity is then tested against the just-calculated value of the exchange coefficient. The motivation behind this test is as follows: It may be seen from

$$K = \{kz(1-\beta R_i)\}^2 \frac{\partial S}{\partial z} \quad (G2.53) \quad (28)$$

that the exchange coefficient will decrease as the Richardson's number increases (i.e., as the lapse rate becomes more stable or the wind shear diminishes), until $\beta R_i = 1$. For values greater than unity, the exchange coefficient again increases, so that if the forced-convection formula for K (28) is used, very stable conditions such as are frequently observed under surface-based nocturnal inversions would be associated with very large values of K. Such a result is clearly at odds with reality, so an additional convection regime, the "very stable" regime, is employed when $\beta R_i > 1$. The test described above is an indirect way of determining βR_i .

If X is less than the forced-convection exchange coefficient, then the model selects the very stable regime. This regime is characterized by a constant $K = 10^4 \text{ cm}^2 \text{ sec}^{-1}$, and a linear profile of wind. The heat flux is calculated by

$$H_o = -\rho c_p K_{\min} \left[\frac{T_h - T_i}{h - z_i} + \frac{g}{c_p} \right] \quad (G2.80) \quad (29)$$

the 50 m wind speed is set equal to 41% of the geostrophic 50 m wind speed, and the surface wind is evaluated at 10 m from a linear profile decreasing from the 50 m wind speed to zero at the surface.

If X is greater than the forced convection exchange coefficient, implying that $\beta R_1 < 1$, then the forced convection formulation is used. The 50 m wind speed is calculated by use of

$$S_h = \frac{u_*}{k} \ln(h/z_0) + \frac{u_*}{\theta_*} \frac{\beta g}{\theta} (h - z_0) \quad (G2.55) \quad (30)$$

and the surface wind speed is evaluated assuming a logarithmic profile law below anemometer level (10 m).

There remains one more possibility - that A is negative, but less than B in absolute value. Such a situation would obtain for small, negative Richardson's number; i.e., slightly superadiabatic lapse rate and large wind shear. In such a case, the heat flux is recomputed from the free convection formula (19). A comparison is made of the heat flux calculated both ways; the appropriate convection regime is selected on the basis of which formulation yields the largest numerical value for the heat flux.

Finally, at the end of the routine, the values calculated in (12) and (13) are multiplied by the 50 m wind speed, thus producing u_e and v_e components of the anemometer level wind. As a last step, the values of the computed eddy exchange coefficients are checked to be within the range

$$10^4 \text{ cm}^2 \text{ sec}^{-1} \leq K \leq 10^4 \text{ cm}^2 \text{ sec}^{-1}.$$

Any values outside this range are set equal to the limiting values.

At this point, we have temperature and specific humidity at each level, we have diagnosed geostrophic winds corrected by the thermal wind term, and we have calculated the eddy viscosity at 50 m. It is now necessary to modify the geostrophic winds according to Ekman theory.¹⁸

First, the difference $U_h - u_g^h$ between the actual 50 m wind and the geostrophic 50 m wind is computed. The parameter α defined by

$$\alpha = \left(\frac{f}{2K_m} \right)^{1/2} \quad (G2.19) \quad (31)$$

is computed, using the value of K_m computed previously for the appropriate convection regime. Then, the diagnosed wind components at each level are

¹⁸Subroutine HORWIND.

obtained by solving

$$u = u_g + e^{-\alpha(z-h)} \{ [U_h - u_g^h] \cos[\alpha(z-h)] + [V_h - v_g^h] \sin[\alpha(z-h)] \} \quad (G2.24) \quad (32)$$

and

$$v = v_g + e^{-\alpha(z-h)} \{ [U_h - u_g^h] \sin[\alpha(z-h)] - [V_h - v_g^h] \cos[\alpha(z-h)] \} \quad (G2.25) \quad (33)$$

It should be noted that the 1600 m geostrophic winds are also modified in this process, but by a very small amount, since the exponential factor $e^{-\alpha(z-h)}$ is very small for $z=H$ (1600 m).

This step completes the diagnosis of the horizontal wind field. We must now determine, from the wind field, the fields of terrain-induced and frictionally-induced vertical motion.¹⁹ The terrain-induced vertical motion \hat{w} is first calculated by a finite-difference approximation to

$$\hat{w} = m \left\{ u \frac{\partial E}{\partial x} + v \frac{\partial E}{\partial y} \right\} \quad (G2.34) \quad (34)$$

where E is terrain elevation. Upstream finite differences are used to approximate the gradient. We will digress at this point to describe how the upstream point is determined.²⁰ First, the sign of the u -component is tested. If u is negative, meaning that the mapped flow has a component from the east,

$$\begin{array}{ccccc} u \text{ positive} & & u \text{ negative} & & \\ & \rightarrow & & \leftarrow & \\ \cdot & & \cdot & & \cdot \\ \ell-2 & \ell-1 & \ell & \ell+1 & \ell+2 \end{array}$$

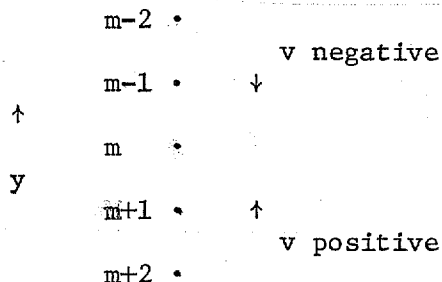
then the upwind point is selected as point $(\ell+1)$; if positive, point $(\ell+1)$ is selected. If point ℓ is on the boundary, and the u -component is such as to indicate inflow, then the upwind point is selected as point ℓ itself, so that the gradient of the advected quantity will be zero.

Similarly, the sign of the v -component is tested. If v is negative, meaning that the mapped flow has a component from the north, then the up-stream point selected is the point immediately north of the gridpoint at which an estimate of the gradient is desired. However, a note should be made here of a peculiarity of the indexing system employed by the Air Force. Although the coordinate system is right-handed, so that the x -coordinate

¹⁹Subroutine WINDUP.

²⁰Function LADVC.

(denoted by the position index ℓ) increases from left to right and the y-coordinate increases from bottom to top, the y-coordinate position index m increases from top to bottom. Thus, the indexing for the y-derivative differs from that customarily encountered. For v negative, then



the upstream point is ($m-1$). Again, if m is at a boundary, and inflow is indicated, the upstream point is m itself.

Next, the frictionally-induced vertical motion w is calculated by solving

$$w(z) = -m \int_h^z \left(\frac{\partial u}{\partial x} + \frac{\partial v}{\partial y} \right) dz, \quad (G2.32) \quad (35)$$

which is the integral of the continuity equation. This calculation is done over the interior only; w is set to zero on the lateral boundaries. Standard centered-differences are used to approximate the divergence:

$$\nabla \cdot \vec{V}_k = \frac{m}{2\Delta x} \{ u_{\ell+1,m,k} - u_{\ell-1,m,k} + v_{\ell,m-1,k} - v_{\ell,m+1,k} \} \quad (36)$$

Finally, the integral in (32) is approximated by the trapezoidal rule and the vertical motion determined based on $w_h=0$.

The mixing coefficients at the top of the contact layer have previously been computed.²¹ This calculation for the heat and moisture coefficients must now be extended to the remaining levels.²² The difference between the lapse rate and the dry adiabatic is calculated for each level above 50 m,

$$A_k = \frac{T_k - T_{k-1}}{z_k - z_{k-1}} + \frac{g}{c_p} \quad (37)$$

²¹This was done in subroutine STRAB.

²²Subroutine MIXCOF.

This is equivalent to the gradient of potential temperature. Note that the gradient actually applies to the layer below level k; the calculations are done for k=2,3,4,5,6,7. Also, the quantity

$$P_k = (u_k - u_{k-1})^2 + (v_k - v_{k-1})^2 \quad (38)$$

is calculated; these two quantities form the important elements of the Richardson's number.

At this point A_k is tested for negative or zero values. If the lapse rate is adiabatic or superadiabatic, A is zero or negative, and a decision between free- and forced-convection must be performed. If $P_k=0$ (no wind shear), the free-convection eddy exchange coefficient is used, eqn. (26). If $P \neq 0$, then the quantity

$$(\beta R_i)_k = \beta \frac{g(\Delta z)^2}{\theta} \frac{A_k}{P_k} \quad (39)$$

is computed. In this case, $\beta R_i < 0$, since $A < 0$. The quantity βR_i is then tested against 0.038, which effectively inquires whether $R_i < -0.03$, Priestley's critical Richardson's number. If so, then the free convection formulation (26) is used; if not, the forced convection equation (28) is employed.

Now if A is positive, meaning that the lapse rate is less than adiabatic, again P is tested for zero values. If $P=0$, the exchange coefficient is set at $10^4 \text{cm}^2 \text{sec}^{-1}$. This indicates that the very stable regime has been selected. If $P \neq 0$, then βR_i is calculated as above and tested against unity. If

$$(1 - \beta R_i) < 0,$$

then the very stable regime is selected, and $K=10^4 \text{cm}^2 \text{sec}^{-1}$. If the inequality is not satisfied, then the forced convection formulation is used.

Finally, all values of K are required to lie in the range

$$10^4 \text{cm}^2 \text{sec}^{-1} \leq K \leq 10^6 \text{cm}^2 \text{sec}^{-1} .$$

With the calculation of the mixing coefficients, we have now available diagnosed winds and vertical motions, temperature, specific humidity, and eddy exchange coefficients for all levels and grid points. Before starting the actual marching process, we need only to compute the vapor flux.²³

²³Subroutine STABVF.

The appropriate stability regime determines which formulation is used. If it is forced convection, the exchange coefficient is first tested for values greater than $10^4 \text{ cm}^2 \text{ sec}^{-1}$; if this is the case, the vapor flux $u_* q_*$ is calculated by solving

$$q_h = q_i + \frac{q_*}{k} \ln \left(\frac{h}{z_i} \right) + \frac{\beta g}{\theta} \frac{q_* \theta_*}{u_*^2} (h - z_i) \quad (\text{G2.57}) \quad (40)$$

If $K=10^4 \text{ cm}^2 \text{ sec}^{-1}$, the very stable regime is selected, and $u_* q_*$ is calculated directly from

$$K \frac{\partial q}{\partial z} = u_* q_* \quad (\text{G2.52}) \quad (41)$$

assuming K is constant with height. Finally, if free convection is the appropriate regime, then the vapor flux is obtained by solving

$$q_h = q_i - \frac{3u_* q_*}{\lambda^{2/3} |u_* \theta_*|^{1/3}} \left(\frac{\theta}{g} \right)^{1/3} \left(h^{-1/3} - z_i^{-1/3} \right). \quad (\text{G2.71}) \quad (42)$$

This completes the steps necessary to begin the marching process.

The first step in that process is to calculate values of surface temperature and surface specific humidity²⁴ for time $t+\Delta t$. Basically, the surface temperature is allowed to change through horizontal advection, including an adiabatic correction to account for the "horizontal" surfaces actually following the terrain, and through radiation. The surface specific humidity is allowed to change principally through advection. However, after the "new" values are computed, an adjustment is permitted to both temperature and specific humidity due to phase changes in water substance.

The first part of the subroutine is devoted to calculating the radiational temperature change. In the AFGWC version of the code, the radiational temperature change was calculated by

$$\left(\frac{\partial T}{\partial t} \right)_R = A_1 \left[\sin \pi \left(\frac{t - \Delta t + 3}{12} \right) - \sin \pi \left(\frac{t+3}{12} \right) \right] \quad (43)$$

where

- t = local time in hours
- Δt = time step in hours
- A_1 = climatologically-determined amplitude of the diurnal temperature wave, available for each grid point and each month.

²⁴Subroutine TMPNXT.

This formulation yields the minimum temperature at 3 a.m. LST and the maximum temperature at 3 p.m. LST, without regard to latitude or season. We have replaced this diurnal wave with another one, also very simple, but which does account for the length of day. The modified diurnal wave is

$$\left(\frac{\partial T}{\partial t}\right)_{RD} = 2A_1 \left[\sin \frac{\pi}{2} \left(\frac{t}{L-2} \right) - \sin \frac{\pi}{2} \left(\frac{t-\Delta t}{L-2} \right) \right] \quad (44)$$

for daytime, where

t = local time after sunrise, in hours
L = local length of day.

A linear cooling rate is prescribed at night:

$$\left(\frac{\partial T}{\partial t}\right)_{RN} = -2A_1 \left[\sin \frac{\pi}{2} \left(1 + \frac{2}{L-2} \right) \right] \left(\frac{\Delta t}{24-L} \right) \quad (45)$$

In these formulae, A_1 is the same as in the AFGWC formulation, so that the diurnal range of temperature is the same for both. The modified formulation yields the minimum temperature at sunrise, and the maximum temperature two hours before sunset. The bracketed quantity in the expression for the cooling rate accounts for the slight cooling which occurs during the two hours prior to sunset.

The first problem is to calculate various time parameters, including local time, sunrise, and length of day. The basic initial time parameter, ITIME, is either 1200Z or 0000Z, and is entered into the code through the date-time group on the initial analysis tape. ITIME is converted to Eastern Standard Time in seconds,

$$TIME0 = \left(\frac{ITIME}{100} - 5 \right) 3600,$$

and the operating time counter, TIME, is initially set to TIME0. The initial calculation is the function

$$P = (1 - \tan^2 \delta \tan^2 \phi)^{\frac{1}{2}} \quad (46)$$

where δ = solar declination angle ($\tan \delta \equiv C3$ in program)
 ϕ = latitude.

P is then used in the formula for local sunrise time,

$$RS = G \pm \frac{12}{\pi} (1-P)^{\frac{1}{2}} (1.5707288 - 0.2121144P + 0.074261P^2 - 0.0187293P^3) \quad (47)$$

The positive sign is taken in winter, the negative sign in summer. It is not clear where the expression for sunrise comes from. From the Smithsonian Meteorological Tables, we glean a formula for the solar altitude (above the horizon),

$$\sin a = \sin \phi \sin \delta + \cos \phi \cos \delta \cos h, \quad (48)$$

where a = solar altitude (elevation above the horizon)
 h = hour angle.

At sunrise, $a = 0$, so one may solve for h ,

$$h = \arccos \left(- \frac{\sin \phi \sin \delta}{\cos \phi \cos \delta} \right). \quad (49)$$

It would therefore appear that eqn. (47) is most likely a series expansion for the arc cosine function.

In any event, once the time of local sunrise has been determined, the lengths of day and night, and the time after sunrise at each step are easily calculated. The radiational temperature change may then be computed as outlined above. However, the magnitude of the change is scaled down depending on the presence of clouds. The impact of cloudiness on the radiational temperature change is parameterized as follows:

For each grid point, the estimate of cloudiness in the free air contained in array DCLD is placed in the variable CLD. It will have the value 1, 2, or 3. Next, the relative humidity at each level from 300 m through 1600 m is calculated and tested against a threshold value, 95%. The levels where the relative humidity exceeds 95% are assumed to be cloudy and their total number is counted. It will be noted that the surface, 50 m, and 150 m levels are excluded; i.e., high relative humidity values at 150 m and below are not allowed to affect the radiational temperature change. It is not clear that this is a good idea.

Now, if there are no clouds (no levels with $RH > 95\%$) at 300 m through 1600 m, the estimate of free air cloudiness is restricted to be no greater than 2. For each cloudy level of the five upper levels considered, CLD is augmented above 2 by 0.2; so that if all five are cloudy, CLD becomes 3. If only four, $CLD = 2.8$, and so on. Once CLD has been determined, then the radiational temperature change is scaled down, if $CLD > 1.0$, by

$$\left(\frac{\partial T}{\partial t} \right)_R (\text{scaled}) = \frac{1}{CLD(CL D - 1.0)} \left(\frac{\partial T}{\partial t} \right)_R. \quad (50)$$

The magnitude of the scaling ranges from 50% for CLD=2, down to 17% for CLD=3. This scaling function differs appreciably from that used by AFGWC,

$$\text{Scaling} = \frac{1}{\text{CLD}^{-1.5}} \quad (51)$$

which ranges from 40% for CLD=2 down to 4% for CLD=3. Experiments have indicated that the 4% scaling almost completely damps out the diurnal wave; for example, for a daily range of temperature of 20°C, under clear skies the scaled range with CLD=3 would be only 0.8°C; whereas with the modification we have introduced, the scaled range would be 3.4°C, which we believe to be somewhat more realistic.

It is abundantly clear that this parameterization is highly arbitrary, and may lead to peculiar results. A significant development effort is needed in order to improve the specification of radiational temperature change, under any cloudiness conditions.

The advective temperature change is calculated using upwind differences, as explained previously, using as an advecting wind the estimate of the anemometer-level wind speed. Wind direction is assumed invariant between anemometer level and $z=h$ (50 m). The remaining part of the temperature change is the adiabatic term $\hat{w}(\frac{\theta}{C})$. All three components of the surface temperature change are then added to the current surface temperature to obtain the forecast at the next time step.

Similarly, the advective change in surface specific humidity is calculated using upstream differences and the anemometer level wind, and added to the current value to obtain the forecast at the next time step.

With the new values of surface temperature and humidity calculated, interrogation as to possible supersaturation is performed. Saturation specific humidity at the new temperature is first calculated, and the new specific humidity is compared to the saturation value. If the air is unsaturated, no adjustment is made. If it is saturated, or supersaturated, the change in temperature due to latent heat release is calculated from

$$\Delta T = \frac{T^2(q - q_s)}{5394 - 4.01 \times 10^{-4} T^2} \quad (52)$$

and the amount of vapor to be condensed from

$$\Delta q = -4.01 \times 10^{-4} \Delta T. \quad (53)$$

These formulas were suggested by Fisher and Caplan (1963).

It is possible, principally through numerical truncation error, that Δq might exceed q itself. If $\Delta q > q$, no change at all is allowed for condensation. If $\Delta q < q$, then ΔT is added to T , and Δq is subtracted from q .

Next, the numerical solutions of the temperature, specific humidity, and specific moisture advection-diffusion equations are carried out.²⁵ All previous calculations are designed to produce the fields necessary to carry out these computations.

The eddy fluxes of heat, water vapor, and moisture are computed first. Centered differences are used, except at the upper boundary, where a one-sided approximation is employed. The fluxes are given by

$$\begin{aligned} \text{Heat Flux} = HF = & \left(\frac{T_{k+1} - T_k}{\Delta z_{k+1}} - \frac{T_k - T_{k-1}}{\Delta z_k} \right) \left(\frac{2}{\Delta z_k + \Delta z_{k+1}} \right) K_k \\ & + \left(\gamma + \frac{T_{k+1} - T_{k-1}}{\Delta z_{k+1} + \Delta z_k} \right) \left(\frac{K_{k+1} - K_{k-1}}{\Delta z_{k+1} + \Delta z_k} \right). \end{aligned} \quad (54)$$

The forms of the analogous expressions for the vapor flux and moisture flux are exactly the same, except that $\gamma (= \frac{g}{c_p})$ does not appear. For $k=1$ (50 m), T_{k-1} becomes the surface temperature, $K_{k-1}=0$, and $K_{k+1}=K_k$, with appropriate modification of the denominator in the finite difference estimate of $\frac{\partial K}{\partial z}$. For $k=7$ (1600 m), $T_{k+1}=T_k$, $\Delta z_{k+1} = \Delta z_k$, and $K_{k+1}=K_k$.

The computed fluxes are next checked for extreme limits; it is required that

$$- 10^{-4} \leq \text{Heat flux} \leq 10^{-4}$$

$$- 10^{-7} \leq \text{Vapor, moisture flux} \leq 10^{-7}$$

This requirement is probably necessary in order to insure computational stability with very long time steps, since the diffusion terms are handled explicitly.

Next, the vertical advection of T , q , and R by the frictionally induced vertical motion w is calculated. Again, upstream differences are used:

$$\left(w \frac{\partial T}{\partial z} \right)_k \approx \begin{cases} w_k \frac{T_{k-1} - T_k}{\Delta z_k} & \text{for } w_k > 0 \\ w_k \frac{T_{k+1} - T_k}{\Delta z_{k+1}} & \text{for } w_k < 0 \end{cases}$$

²⁵Subroutine TRQNX

At the upper boundary, with subsidence, the vertical advection is set to zero. Expressions of analogous form are computed for q and R .

In order to calculate the horizontal advection, the upwind grid points must be determined. Then, the forecasts of T , q , and R may be computed:

$$T_k^{n+1} = T_k^n - \Delta t \left\{ u_k \left(\frac{\Delta T}{\Delta x} \right)_{\text{upstream}} + v_k \left(\frac{\Delta T}{\Delta y} \right)_{\text{upstream}} + w_k \left(\frac{\Delta T}{\Delta z} \right)_{\text{upstream}} + \gamma(w+\hat{w})_k + \text{Heat Flux} \right\} \quad (55)$$

The expressions for q and R are analogous, but without the adiabatic term.

After T_k^{n+1} , q_k^{n+1} , and R_k^{n+1} have been computed, q_k^{n+1} and R_k^{n+1} are checked for negative values; if found negative,

$$q_k^{n+1}, R_k^{n+1} = 0.$$

Also, if $R_k^{n+1} < q_k^{n+1}$, R_k^{n+1} is set equal to q_k^{n+1} .

There follow two adjustment procedures, one for lapse conditions and the other for inversion conditions. The former is known as a "convective adjustment" and is performed when the lapse rate between any two layers exceeds a slightly superadiabatic threshold value. The threshold value is

$$\gamma_{a_k} = \gamma \left(1 + \frac{10}{z_k} \right), \quad (56)$$

where z_k is the height in meters above the ground. If the computed lapse rate between any two layers exceeds γ_a , the temperature at the upper one is adjusted toward warmer values so as to make the lapse rate equal to γ_a . The range of γ_a is from 1.2γ at $z=50$ m to 1.0062γ at $z=1600$ m.

As an example, if the 50 m temperature is more than 0.6°C cooler than the surface temperature, the 50 m temperature is increased to make the difference 0.6°C . If this adjustment is such as to make the 50 m temperature more than about 1.6°C warmer than the 150 m temperature, then that temperature is adjusted upward, and so on. In effect, this convective adjustment may act as a diffusion; in fact, it may dominate the effects of the calculated heat flux.

The second adjustment procedure is based on insisting on a maximum strength for surface-based inversions. In particular, the 50 m temperature is allowed to be no more than 2°C warmer than the surface temperature. If

the model computes

$$(T_{50} - T_{sfc}) > .2^{\circ}\text{C},$$

then T_{50} is reduced by 80% of the computed difference $T_{50} - T_{sfc}$; T_{150} is reduced by 50% of the difference, and T_{300} is reduced by 10% of the difference. This procedure prohibits the development of extremely intense surface-based inversions.

These calculations are carried out for all grid points and levels, and when completed, leave only one further adjustment for phase changes of water substance.²⁶

First, the saturation specific humidity at the new temperature T_k^{n+1} is calculated from Tetten's formula (eqn. 2). The changes in temperature and specific humidity due to condensation or evaporation are calculated from eqns. (52) and (53). If $q < q_s$, then an enquiry is made as to whether any liquid moisture is available to be evaporated. If not, no evaporation takes place, and T and q are not adjusted. However, if $R > q$ (evaporable moisture is available), then Δq is tested against the difference $R-q$; in other words, is the available moisture $R-q$ sufficient to allow a change of Δq ? If so, $\Delta q < (R-q)$, and q_k^{n+1} is augmented by Δq , and T_k^{n+1} is reduced by ΔT .

If the difference $R-q$ is insufficient to allow the full change Δq , ($\Delta q > R-q$), then q_k^{n+1} is augmented as much as possible; i.e., $q_k^{n+1} = R-q$, and T_k^{n+1} is reduced by $(R-q)/9.01 \times 10^{-4}$.

If the air is supersaturated ($q > q_s$), then Δq is negative, and a test is performed to ensure that $\Delta q < q$; that is, no attempt is made to condense more specific humidity than is available. This should not happen, except as a result of numerical truncation errors in very cold, dry air. However, if $\Delta q > q$, then the temperature is augmented by

$$T_k^{n+1} = T_k^{n+1} + \Delta q / 4.01 \times 10^{-4} \quad (57)$$

and q_k^{n+1} is set at a very small minimum value, 0.5 g/Kg.

For the more usual case of $\Delta q < q$, q_k^{n+1} is reduced by Δq , and T_k^{n+1} is augmented by ΔT .

These computations complete one time step. The entire procedure is then repeated to march forward in time.

²⁶Subroutine PHZCHG.

3. Analysis Model

a. Purpose

The purpose of the analysis program is to provide initial input data and hourly boundary conditions for the planetary boundary layer model. Specifically, this information includes temperature (T) and specific humidity (q) at each of eight model levels shown in Fig. 2, an estimate of cloudiness (DCLD) and a parameter (WETT) that simulates surface moisture. The hourly boundary conditions consist of 24 sets of wind components (u and v) and cloudiness defined on the top level of the model. All fields are carried on a 29 x 27 subset of the NMC North American fine-mesh window. The location of the boundary layer grid within the window is illustrated in Fig. 1.

The philosophy behind the analysis is similar to that followed by Hadeen (1970) in the AFGWC version. In essence, the analysis proceeds upward from the data dense area at the surface to the relatively sparse data region aloft. Except at the surface, actual values of temperature and humidity are not analyzed directly at each level, but are specified by a lapse rate analysis anchored at the ground by a detailed surface analysis. Analyzing lapse rates makes it easier to control vertical stability and eliminates any systematic errors in the upper-air observations.

Upper-air data is obtained from conventional land-based soundings, while surface data are taken from both land and ship reports. The first guess fields come from initial and analyzed LFM fields available on permanent files. Finally, boundary conditions at the interface between the boundary layer and the free atmosphere are derived from hourly dumps of the operational LFM forecast.

b. Organization

The analysis package can be broken up into the four principal areas shown in Fig. 3. First, the main program acts as a supervisor coordinating the work of the subroutines and handling peripheral operations such as smoothing, final error checking and output. Second, the bulk of the package consists of subroutines that retrieve information from the permanent files and put it into a form that is palatable to the analysis routine. Third, the analysis section itself includes two routines that determine the optimum initial scan radius for each report and produce gridded fields from scattered observations. Fourth, a single subroutine generates the boundary conditions which are used to drive the forecast model.

The analysis tape that is ultimately sent to the model contains all the necessary information needed to begin a forecast. This information is organized in two files according to Table 1.

c. Procedure

(1) Setting up House.

Prior to entering the main body of the program, certain preliminary duties must be performed in the dayfile. First, the binary program is loaded into core from the library tape. Then a local file is created by copying the LFM forecast dump tape onto disk. After these tapes have been returned, the analysis tape is mounted and the first file containing the station dictionaries and the fixed fields is copied onto disk for latter use. The analysis tape is now positioned to accept the output from the analysis. After all other necessary files are attached, the program is ready to roll.

(2) Supervising the Analysis.

The inner working of the analysis package can best be examined from the point of view of the main program, appropriately called SUPER. The first order of business is to read the upper-air dictionary from the scratch disk and begin the lapse rate analysis.

(3) Upper-air First Guess.

The first-guess lapse rates for the upper-air analysis are generated by subroutines ALFM and GUESS. ALFM retrieves the following analyzed and initial LFM fields from permanent files FMANL and FMOO, respectively:

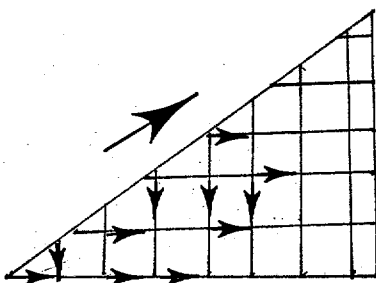
<u>FMANL</u>	<u>FMOO</u>
Sfc. temp	Sfc. pres.
0.0 bdy - 1.0 bdy R.H.	1.0 bdy - 0.3 trs R.H.
1000 mb ht.	1000 mb temp. & dewpoint
850 " "	850 " " "
700 " "	700 " " "
500 " "	500 " " "
	500 " u & v
	1524 m "
	1829 " "
	2134 " "
	2743 " "
	3658 " "

All fields on FMANL are carried on the 3021 point fine-mesh grid (53 x 57), while fields on FMOO are restricted to the 1977 point fine-mesh octagon (see Fig. 1).

This latter arrangement leads to problems because the lower right-hand corner of the PBL grid protrudes out of the octagon. In order to fill this area with data, the parameters along the lower right diagonal of the octagon are faded into the corner using the averaging scheme

$$\phi_{i,j+1} = \frac{1}{2}(\phi_{i,j} + \phi_{i-1,j+1}) \quad \begin{cases} i = 27, 21 \\ j = 23, 29 \end{cases}$$

in a sequence this resembles the building of a pyramid as illustrated below.



Although this appears to be a rather heavy-handed method of extrapolation, the meteorological fields in this geographical region are sufficiently smooth that the loss of detail caused by the averaging scheme is not believed to introduce any serious errors. At any rate, this problem can only be eliminated by rewriting the operational post-processor to output all fields over the fine-mesh rectangle. This modification, by the way, is also a prerequisite for any future expansion of the boundary layer window.

Subroutine GUESS is called upon to convert the fine-mesh fields to appropriate units and calculate first guess lapse rates in each model layer. The conversions include changing the base of temperature from Kelvin to Centigrade and that of height from above-sea-level (ASL) to above-ground-level (AGL). Also, dewpoints are converted to specific humidity according to the equation

$$q = \frac{0.62e}{(p-0.38e)} \quad (58)$$

where the vapor pressure, e , is found using the formula

$$e = 6.11 \times 10^{\frac{7.5 T_D}{T_D + 237.3}} \quad (59)$$

Additional accuracy could be obtained if the constants appearing in the exponent were modified over water. At the surface, dewpoints are not available directly but must be inferred from surface temperature and boundary layer relative humidity.

First guess lapse rates are found by interpolating temperature and specific humidity to each model level and then computing vertical gradients. The interpolation takes the form

$$\phi_{\ell} = \phi_K + \frac{\phi_{K+1} - \phi_K}{Z_{K+1} - Z_K} (Z_{\ell} - Z_K) \quad (60)$$

For all model levels, ℓ , (except the surface) such that $Z_K < Z_{\ell} < Z_{K+1}$, where K represents isobaric levels, in descending order of pressure and also the surface (whenever it falls in the sequence). The uppermost model level ($\ell=8$) is generally between 850 mb and 700 mb. However, in cold air over high terrain, the 700 mb level may be below the top of the model (in some instances below ground level) and this necessitates working with 500 mb fields in order to avoid extrapolation from below. An example of the location of the vertical structure of the model with respect to the fine-mesh fields is shown in Fig. 2.

Layer lapse rates are computed from interpolated parameters by

$$\frac{\Delta\phi}{\Delta Z} = \frac{\phi_{\ell+1} - \phi_{\ell}}{Z_{\ell+1} - Z_{\ell}} \quad (61)$$

This technique usually produces reasonable lapse rates, except over high terrain in situations where there are strong horizontal temperature gradients. In such cases, computed lapse rates tend to be noisy and somewhat unstable. To counteract this tendency, all negative lapse rates are limited to the dry adiabatic value; there is no restriction on positive lapse rates.

Referring to Fig. 4, it is obvious that the first guess vertical structure contains very little detail because of the small depth of the model compared to the spacing of the mandatory levels. This lack of detail is unfortunate, especially over the oceans where the absence of upper-air data makes further improvement of the analysis impossible. One result is that the high moisture content of the air just above the sea surface tends to be reflected all the way to the top of the model by the rather bland humidity lapse structure. This overspecification of the initial moisture distribution has catastrophic effects on a nonprecipitating forecast model, especially in regions, such as the west coast, that are influenced by large scale on-shore flow. A solution to this problem may be found in the use of satellite-derived soundings and models of vertical

Table 1.

	Parameter	Units	Storage	Description
Upper-air Dictionary	Call	-	121 6-word Records	Call Letters
	NB	-		Block Number
	NS	-		Station Index
	GI	-		I-index
	GJ	-		J-index
	ELST	M.		Station Elevation
LFM Terrain	E	M.	784-word Record	Model Terrain Elevation
Surface Dictionary	NB	-	715 5-word Records	Block & Station No.
	Call	-		Call Letters
	GI	-		I-index
	GJ	-		J-index
	TCOR	°C		Adiabatic Temperature Correction
PBL Fixed Fields	Zφ	CM	783-word Record	Roughness Length
	SLONG	Degrees	1566-word Record	Longitude
	SLAT	-	12	Latitude
	AONE	-	784-word Record	Radiation Coefficients
Initial Fields	U	M./Sec.	783-word Record	X-component
	V	M./Sec.	"	Y-component
	DCLD	-	"	Cloudiness
	WETT	-	"	Surface Wetness
	T	°C	8 783-word Rec.	Temperature
	RH	-	"	Relative Humidity
Boundary Conditions	KOUNT	Hours	24	Time Counter
	DCLD	-	2350-word Records	Cloudiness
	U	M./Sec.		X-component
	V	M./Sec		Y-component

humidity distribution based on surface observations of cloudiness. In the meantime, users of the forecast model will have to contend with a severe wet bias in the western United States.

The first guess out of the way, ALFM has one more task to complete - the calculation of the initial hour wind field at the top of the model. After the initialized wind fields are read from FM00, subroutine AWIND determines where the topmost level lies with respect to the fine-mesh fields and then performs a linear interpolation of u and v to that level.

Before proceeding with the upper-air analysis, SUPER makes an estimate of initial cloudiness using the tropospheric relative humidity passed through common by ALFM. Cloudiness (DCLD) is defined on an integer scale of 1 to 3 where

Mean RH	DCLD	Description
0-50	1	Clear or scattered
51-80	2	Broken
>80	3	Overcast or obscured

This parameter is used to modify the amplitude of the diurnal temperature wave in the forecast model.

(4) Upper-air Data.

Next in line are the data processing routines, ACCESS, AMESH, and ALAPSE. These are in charge of opening and reading data from the ADPUPA file, screening the information for errors, arranging mandatory and significant levels in ascending order and computing model lapse rates.

Unlike the random files which require searching a table of contents to find a desired field, the data files ADPUPA and ADPSFC are written in sequential order according to the block and station number of the incoming reports. This arrangement greatly simplifies the job of selecting those reports that are found in the upper-air dictionary.

As each report is read from the data file, it is checked to see if: it is a land-based sounding, was taken within three hours of the synoptic time and corresponds to an entry in the dictionary. If a particular report passes all the tests, it is ready for the mill.

First, mandatory level data is stored in four word groups consisting of pressure, geopotential, temperature and dewpoint. The same thing is done with the significant levels except that geopotential is replaced by station elevation as the former is not transmitted.

This completed, AMESH is called to knead the data into a more workable form. Mandatory level data is checked to see if the information at each level is complete. If one or more of the parameters are missing, that particular level is discarded. Furthermore, each level is checked internally for dewpoints greater than $\pm 100^{\circ}\text{C}$ (as in the case of motor boating) and negative geopotentials (usually an error in the transmission of the sign). If a level survives the gantlet, its dewpoint is replaced by specific humidity and the program proceeds to the next level.

When the mandatory levels have been exhausted, a similar battery of tests is performed at each significant level, with one exception. If any of the surface parameters are missing, the surface and all subsequent levels are thrown out. Later, in subroutine ALAPSE, the missing surface data is restored by interpolation from fine-mesh surface fields in order to connect the mandatory levels to the ground. As a substitute for direct surface observations, however, this is not considered accurate enough to justify retaining other significant levels whose heights would ultimately depend on surface values.

As soon as the significant level data is deemed fit for consumption, dewpoints are replaced by specific humidity and the height of each level is computed from

$$z_{\ell+1} = z_{\ell} - \frac{R}{2g} (T_{v\ell+1} + T_{v\ell}) \log_e \frac{P_{\ell+1}}{P_{\ell}} \quad (62)$$

where ℓ indicates the levels in ascending order and T_v , the virtual temperature is given by

$$T_{v\ell} = (T_{\ell} + 273.5)(1 + 0.61 m_{\ell}) - 273.5; \quad (63)$$

the mixing ratio, m , is simply

$$m = 0.62e/(p-e). \quad (64)$$

At this point, the mandatory and significant level data are meshed in order of ascending height and stored in array RAOB. The meshing process is stopped as soon as the first level above 1600 m AGL is reached. Control is then passed back to ACCESS which fetches the next report and so on until all appropriate reports have been similarly processed.

SUPER now calls subroutine ALAPSE which takes the ordered data stored in RAOB and interpolates temperature and specific humidity to the model levels using the method previously employed by the first guess routines. Here, an internal consistency check is made that limits the value of negative temperature lapse rates to

$$\frac{\Delta T}{\Delta z}_{lim} = \Gamma_D + \Gamma_A / (1 + l^2) \quad (65)$$

where $\Gamma_D = -9.75 \times 10^{-3}$, the autoconvective lapse rate, $\Gamma_A = -3.42 \times 10^{-2}$ and l is the model layer number (1-7). This cutoff value, devised by the Air Force, allows very unstable conditions near the ground but approaches the dry adiabatic value at the top of the model. As with the first guess fields, there is no limit on positive lapse rates because very strong surface inversions are frequently observed, especially in the morning analysis. Unfortunately, there is no way to screen errors in the transmissions of the sign of the temperature which leads to spurious (and unrealistically large) positive lapse rates.

Fig. 5 shows an example of a processed sounding and illustrates the smoothing effect of interpolating raw data to fit the model structure. In the future, it may be possible to devise a scheme whereby significant features such as frontal inversions and shallow layers of high humidity (as in low cloud decks) would be weighted to increase their influence on the analysis. As it stands now, even the relatively fine vertical structure of the model cannot resolve such features satisfactorily.

Another problem that has cropped up (at the observational end of the system) is the fact that many stations frequently transmit little, if any, significant level data. Indeed, if only mandatory data is available (RADAT data), the report has no more detail than the first guess. The only solution to this problem is to require additional measurements within the lowest 2000 m of the radiosonde ascent.

(5) Lapse Rate Analysis.

The actual analysis is carried out by subroutines ASCAN and ANAL. Called from SUPER, ASCAN determines the initial radius of the influence area for each report based on the density of other reports in the vicinity. Starting at two grid lengths, the radius is incremented by one grid length until the data density criterion is satisfied. This criterion is met when

$$\sum_{i=1}^n (R-d_i) \geq 2R$$

where n is the number of reports within an area of radius R_K and d_i is the distance between the central report and one of the surrounding reports. The maximum radius allowed is seven grid lengths.

Subroutine ANAL incorporates a modified Barnes (1964) technique to obtain gridded fields from scattered data points. First, a bilinear interpolation is used to compute the value of the first guess at each report position. Then the difference between this and the observed value is spread to each grid point within the influence area and weighted according to the distance, d , between each grid point and the report position. The weight is given by Cressman's (1959) function

$$W = \frac{R^2 - d^2}{R^2 + d^2} \quad (66)$$

After all reports have been considered, the sum of the weighted differences at each grid point is divided by the number of reports, n , influencing that point, i.e.,

$$A_{i,j} = \frac{1}{n} \sum_{k=1}^n W_K (\phi_{K_{\text{GUESS}}} - \phi_{K_{\text{OBS}}}) \quad (67)$$

The matrix, A , represents a change field that is added to the first guess to improve the analysis. Two more passes are made with the scan radii reduced by 0.6 each time.

The choice of the weighting function, the method of determining initial scan radii and the degree of reduction after each scan were arrived at rather arbitrarily. Further study is required to determine the optimum parameters for handling data of this particular type and density.

(6) Surface Analysis.

The surface analysis is perhaps the most critical part of the entire program because it serves as an anchor for the analysed lapse rates and ultimately determines the absolute structure of the initial fields. In order to take advantage of the abundance of surface observations both on land and from ships, the surface analysis is carried out over an area that extends six grid lengths beyond the PBL window in all directions. This extension is possible because the fine-mesh surface fields used for the first guess are available over the LFM rectangle.

Subroutine SURF handles all the guess and data processing by itself. The guess fields are derived from mean sea level

pressure, surface temperature and boundary layer relative humidity on FMANL, while the LFM terrain is obtained from permanent file FIXFLD. Surface pressure is calculated by

$$P_{\text{sfc}} = P_{\text{msl}} e^{\frac{-gZ_m}{RT}} \quad (68)$$

The quantity, \bar{T} , is defined as

$$\bar{T} = T_{\text{sfc}} + \frac{gZ_m}{4c_p} \quad (69)$$

and represents a crude estimate of the mean temperature in the imaginary layer of air between sea level and the terrain height, Z_m . The pressure is used immediately to compute surface specific humidity and is saved for later use as a back-up in case pressure is missing from a report.

Surface data is pulled off of ADPSFC in the same manner as upper-air data. Besides the error tests described previously, a number of additional checks are made. If a reported temperature deviates from the first guess by more than 15°C, the entire report is discarded. Also, if the temperature-dewpoint spread exceeds 25°C, the dewpoint is ignored. In general, there are more temperatures than humidities available to the analysis.

The limit on temperature-dewpoint spreads sometimes causes the program to throw out good data in the southwest during dry spells. However, it eliminates errors that arise from faulty transmission of the sign of the spread and also weeds out Mexican reports which frequently flag a missing spread by sending a value that will produce a dewpoint of -20°C instead of the standard 99999.0. In order to make this test more sensitive to regional idiosyncrasies, it might be possible in the future to use a variable criterion in this test.

The reported station pressure is not accepted if it exceeds 1060 mb - a situation that occurs with stations that routinely omit this parameter ($p = 99999.0$) and whenever there is a misplaced decimal. If station pressure is not available, it is calculated from reported sea level pressure or the fine-mesh sea level pressure.

Once the surface dictionary is exhausted, ship reports are read from the data file. To determine if a ship lies within the extended region, its position in grid coordinates is computed from reported

latitude and longitude. If the ship is in the ball park, its position is tested against the terrain elevation at the nearest grid point. On occasion, a ship will report a position that places it in a desert or on top of a mountain range. Many times, ships anchored in port will flunk this test because the elevation is not zero. This is actually a blessing in disguise because most large ports send conventional land-based observations and it would be unfortunate if these reports were spoiled by ship stations whose reputation for accuracy is not particularly esteemed.

When all reports are in, a special correction is added to the temperature and dewpoint data. Each station has a unique correction which is defined by

$$C = - \frac{g}{c_p} (Z_m - Z_{stat}) \quad (70)$$

and represents the adiabatic temperature difference between the model terrain and the station elevation. In effect, this term adjusts the station report to make it compatible with the model terrain. The forecast model forces the wind to follow the terrain but compensates for this restriction with an orographic temperature tendency,

$$\frac{\partial T}{\partial t} = \hat{W} \frac{g}{c_p} \quad (71)$$

where

$$\hat{W} = u \frac{\partial Z_m}{\partial x} + v \frac{\partial Z_m}{\partial y} \text{ is the terrain-induced vertical velocity.}$$

The correction reduces the error produced by this tendency term in regions where there is a large discrepancy between true and model terrain. It should be noted that the correction must be applied in reverse when looking at forecast fields.

Although the correction procedure conserves thermal energy (θ is constant), it wreaks havoc on specific humidity when it is computed using corrected dewpoints. This effect is annulled, however, when relative humidities are calculated with saturation values derived from corrected temperatures.

(7) Final Processing.

The surface data is finally sent to the analysis routines and the resulting gridded fields are smoothed using a 49-point filter devised by Gerrity. Smoothing is detrimental to a division field

like relative humidity because it upsets the delicate balance between temperature and specific humidity. However, this particular filter is the best way to remove the noise introduced by the analysis scheme without annihilating significant meteorological scales.

Starting with the surface analysis, the temperatures and specific humidities are generated for each level in succession by

$$\phi_{l+1} = \phi_l + \frac{\Delta\phi}{\Delta z} (z_{l+1} - z_l). \quad (72)$$

Relative humidities are computed at each level to make sure that the calculations do not produce any negative or super-saturated values.

When the build-up is finished, the smoother is applied to each level. This procedure tends to modify the analyzed lapse rates by independently varying parameters at two different levels. It might be more consistent with the philosophy of the analysis to smooth the lapse rates before the build-up process is started. At any rate, the need for further investigation in this area is indicated.

Before the fields are written onto the analysis tape, a parameter called WETT, which acts as a source of water vapor at the ground, is calculated from

$$WETT = \frac{q_{50} - q_{sfc}}{q_{sfc} - q_{sfc}^{(sat)}} \quad (73)$$

If a positive humidity lapse rate exists in the lowest model layer, this parameter becomes negative. In such cases, it is automatically set to zero. It is made equal to 1.0 over bodies of water because they represent infinite sources of moisture.

(8) Outputting the Analysis.

The analyzed fields are written on tape directly after the initial winds. The output is grouped in eighteen 783-word records, starting with DCLD and WETT and the eight records each of temperature and relative humidity.

The reason that relative instead of specific humidity is sent to the forecast model is that specific humidity is computed by a slightly different method in the forecast model. Specific humidities are recomputed before the forecast is begun by multiplying analyzed relative humidities and saturated specific humidities computed by the technique employed by the forecast model.

(9) Hourly Boundary Conditions.

All that remains to be done is the generation of hourly wind components and cloudiness. These are derived from the winds and precipitable water carried between tropospheric sigma levels in the LFM dump.

The heights of each sigma level are computed from pressure and temperature; wind components between these levels are then interpolated to 1600 AGL. Tropospheric relative humidities are derived from forecast ambient and saturated precipitable water in the three tropospheric layers by the relation

$$\text{R.H.} = \frac{W_1 + W_2 + W_3}{Ws_1 + Ws_2 + Ws_3} \quad (74)$$

The same criteria to determine DCLD in the analysis are used here.

Boundary conditions are written on the analysis tape in a block of 24 records. Each record contains an hour counter (1-24) and 783 words each of DCLD, u and v. This completes the preparation of the analysis tape.

d. Suggestions for Further Research

In this section, an attempt will be made to summarize the known deficiencies in the analysis and to suggest possible remedies and improvements.

The deficiencies can be grouped into four categories:

- (1) Inadequate modeling of the physical parameters with respect to distribution, especially in data sparse regions.
- (2) The choice of restrictions and limits imposed on the data during the process of error checking.
- (3) Errors introduced by the mechanics of the analysis itself.
- (4) Problems external to the analysis, such as lack of quality, density, representativeness, and vertical resolution of the data.

Examples of each type of problem have been mentioned in the text along with a general description of their effect on the performance of the forecast model.

Solutions to these problems will be found along two different, but equally important, lines of investigation. First, there are changes which can be made by taking advantage of information and techniques which are presently available. Second, long range plans should be made to utilize techniques which are proposed or are already in the development stage.

A number of improvements can be made to the modeling of parameters based on climatological considerations and the use of indicators that are directly related to these parameters. For example, in maritime regions, the first guess field could be modified to reflect such phenomena as trade inversions and the trends in seasonal and diurnal low-level stability. The vertical model would then be adjusted by ship observations of sensible weather, cloudiness and condensation pressure spread and also satellite-derived nephanalyses. This technique would go a long way toward eliminating the wet bias on the West Coast. Similar considerations, plus observations of things like the state of the ground, would aid in improving the first guess over continental regions.

With regard to error checking, the cutoff values on the observed parameters should be made sensitive to climatology, latitude, terrain and perhaps even short-range trends in the sensible weather. Thus, observations from desert stations would be treated differently from those taken at stations in mountains, the Great Plains, or the East Coast.

Deficiencies in the analysis technique lend themselves to improvement by statistical methods, which could be used to determine optimum treatment of scan radii, number of scans, weighting, etc. For instance, important features in the humidity field exist at smaller scales than those of temperature. It may be advantageous, therefore, to analyze humidity in a different manner than temperature. The final choice of analysis techniques would depend strongly on the scale of a particular parameter, the density of observations and the quality of the first guess. The same considerations would apply to the choice of filters and the criteria for maintaining internal consistency of the analyzed fields.

A major factor in improving the data itself would be the inclusion of more observations in the permanent files by utilizing reports which are presently available only on teletype. Also, greater vertical resolution could be obtained by increasing the number of measurements taken in the lowest 2000 m of a radiosonde ascent. At present, this is only practiced at EMSU sites and at certain airports and gunnery ranges.

As far as future projects are concerned, the implementation of automatic remote sensing devices such as buoys, and development of a reliable ground-base sounding system (radiometric thermosondes, for example, will be a boon to any analysis of boundary layer phenomena. The prospects of honing this analysis to a fine point are encouraging.

4. Output Section

In the output section, we are attempting to develop products which take advantage of the considerable detail of the low level structure of the model atmosphere with its excellent vertical resolution. In its present form, the capability exists to display any of the dependent variables at any level in a horizontal depiction with more than one field, and including vector winds on a chart. In addition, horizontal depictions of derived quantities, such as divergence, vorticity, stability indices, and a long list of environmental control related quantities such as air pollution meteorological and fire weather control quantities may also be available.

Individual prognostic soundings may be shown and having these available makes possible objective techniques for determining areas of icing, precipitation types, and low level turbulence. Finally, detailed time cross-sections at individual stations are available.

Our output display is produced on microfilm using the Information International FR-80 film recorder at NMC, along with prognostic sounding plotted on computer paper. Currently, we produce the following forecast fields for initial, 12 and 24 hours.

a. Mixing heights and transport wind fields utilizing prognostic sounding available from the forecast model. Two techniques are employed to predict the mixing heights:

(1) For forecasts verifying at 00Z, a scan technique is employed. The model soundings are scanned up to 4 times.

(a) Scan 1. Flags significant surface based inversions ($\Delta P > 10$ mb and $\Delta T > 2^{\circ}\text{C}$) and determines inversion strength- $\Delta P\Delta T$. Regardless of whether a surface based inversion is found or not, we proceed to second scan.

(b) Scan 2. Checks for upper level inversions and flags the base of any inversion found as the mixing height. The strength of inversion is also found ($\Delta P\Delta T$). If no inversion, we proceed to third scan.

(c) Scan 3. Checks for any isothermal layer where ΔT for two consecutive points is $\leq 0.5^{\circ}\text{C}$ and flags the base of isothermal layers as the mixing height. If no inversion is found, we proceed to the fourth scan.

(d) Scan 4. Locates regions where the lapse rate becomes more stable than the moist adiabatic. This is done by first converting

all the temperatures to the pseudo equivalent potential temperature. The base of this layer is defined as the mixing height.

The scanning technique is aborted once a mixing height is found and the average wind within the mixing layer produces the transport wind speed. If no mixing height is found within the model, we print out a 7777 which indicates unlimited mixing.

(2) For forecasts verifying at 1200Z, we use a technique proposed by Summers (1968) and Leahey (1970), which we call the heat added mixing height. When cool air from the surrounding countryside is advected over the warmer urban surface, the air near the urban surface is heated by conduction and an adiabatic mixing layer is related to additional thermal energy from the urban surface, the wind speed and the lapse rate of temperature in the planetary boundary layer, upwind of the city and the city size. The formulation is:

$$h_1 = \left(\frac{2H_1 X_1}{\rho c_p \gamma u} \right)^{1/2} \quad (75)$$

where

P = the density of air (gr cm^{-3}) = 1.3×10^{-3}

c_p = specific heat = $.240 \text{ (cal } ^\circ\text{K}^{-1}\text{gr}^{-1})$

H_1 = average heat output from city = $1 \times 10^{-3} \text{ cal cm}^{-2}\text{sec}^{-1}$

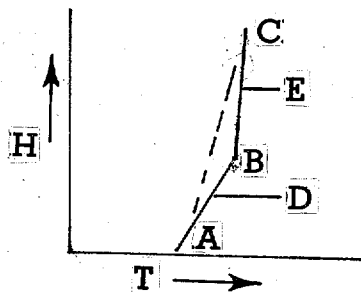
X_1 = distance from edge to center of city

city size - use $\frac{40\text{km}}{2}$ city = 20,000 cm

γ = lapse rate of potential temperature determined by scanning sounding

u = average wind speed through mixing layer.

Note: H_1 and X_1 are fixed fields currently in our program, but can be individualized for each grid point. X_1 is the city size which is a function of wind direction and speed and urban area.



Method: Determine lapse rate A-B put in equation, if mixing height occurs within region D, flag. If not, calculate lapse rate A-C, if mixing height occurs in region E, flag. If not, try scan technique within model. If no mixing height is found, flag as unlimited. Transport wind speed is the mean wind within the mixing layer.

Note: This method is being tested in an attempt to see if we can take into account the effect of the urban environment on the mixing height in contrast to the Miller-Holzworth adiabatic intersection technique.

b. Relative concentrations (\bar{X}/\bar{Q}) are computed for each grid point based on a general dispersion model over urban areas developed by Miller-Holzworth (1967).

Meteorological Potential

Aim: To consider severity of stagnation period.

Tool: General model of dispersion over urban areas (Miller-Holzworth)

Averaged normalized pollutant concentration (\bar{X}/\bar{Q} in sec meter⁻¹)

\bar{X} - The city-wide average concentration in grams meter⁻³ is normalized for the city-wide average area emission rate.

\bar{Q} - Grams meters⁻²sec⁻¹

These are a function of mixing height (H) in meters, and average wind speed (U) meters sec⁻¹ through H and city size (S) in meters, the along-wind distance across the city.

The main assumptions of the model are:

1. Steady state conditions prevail.
2. Emissions occur at ground-level and are uniform over the city.
3. Pollutants are non-reactive.
4. Lateral diffusion is neglected.
5. Vertical diffusion is confined to mixing layer.

Thus, the potential for urban air pollution is considered in terms of meteorological variables; other parameters are treated as constant.

Equation used:

$$\bar{X}/\bar{Q} = 3.613 H^{0.13} + \frac{S}{2HU} - \frac{(.088)(U)(H^{1.26})}{S} \quad (76)$$

The assumed city size $S = 40$ km.

In this manner, dispersion conditions at a specified time and location can be represented by a single number that can be readily compared with relative concentrations for other time periods, locations or with climatological statistics in determining the severity of individual air pollution episodes.

Note: H = city size which can be varied for individual location based on wind direction and speed.

c. Aviation weather guidance materials

(1) 300 m temperature and vertical velocity and a weighted 50-300 m mean relative humidity. Use for ceiling determination below 1000 feet.

Note: Weighted relative humidity - the relative humidity for each level is weighted by the thickness of the layer using

$$RH = \frac{(RH_1 * 1 + RH_2 * 50m + RH_3 * 100m + RH_4 * 150m + RH_5 * 300m + RH_6 * 300m + RH_7 * 300m + RH_8 * 400m)}{1600m}$$

(2) 1600 m temperature and vertical velocity and a weighted 600-1600 m mean relative humidity. Use for ceiling determination between 1000 and 5000 feet.

(3) We are experimenting with determining precipitation types, icing conditions and multiple freezing levels utilizing predicted sounding

profile models produced in the model. Figs. 6-8 illustrate the six profiles available.

Note: We are experimenting with utilizing LFM temperature and pressure fields above the PBL model in order to extend our forecasts of icing and freezing levels above 1600 m (AGL).

(4) Vector wind plots and temperature at 50 m and 1600 m. These charts can be utilized in location of surface and upper air systems along with visual depictions of advection areas and inflow.

(5) Time cross sections which can be tailored for use at individual forecast offices for aviation terminal forecasting and also for air pollution meteorological needs. See Fig. 9. Wind directions are plotted with respect to north and speeds are given in knots by the customary plotting convention. Values of temperature ($^{\circ}\text{C}$) and relative humidity (%) are plotted at each level and each hour. Solid isolines are isotherms at 1°C intervals, and the dashed lines are relative humidity contours in intervals of 10%. Below the diagram are plotted hourly predicted values of surface temperature ($^{\circ}\text{F}$).

(6) Prognostic soundings on Stüve diagrams for individual locations are plotted on computer paper. Fig. 10 is a schematic of a prognostic sounding and possible teletypewriter message, meshed with LFM data.

(7) Severe weather index - Best Lifted Index (BLI), Fujita (1970). The method we are testing consists of lifting each point in the vertical structure of the PBL dry adiabatically to the condensation level (LCL) and then moist adiabatically to 500 mb. The temperature difference between the lifted value and the 500 mb temperature yields a lifted index. The lowest lifted index obtained by this method defines the best lifted index. We analyze the BLI for every 2°C and the pressure of the best lifted index (PBI) every 50 mb. The 50 meter vector wind is also plotted on this chart as an aid in depicting moisture inflow in possible severe weather areas.

Work is progressing in the development of guidance material for the following programs:

A. Fine weather forecasting. Working with the USDA Forest Service, we are testing prediction methods of burning indices and manning levels for the National Fire Danger Rating System (Deeming, et al., 1972).

B. Stagnation area forecasting.

C. Inversion breakup forecasts. Technique to forecast time and temperature needed to break a surface based on upper level inversion.

D. Space cross section forecasts for pilot briefing purposes.

E. Low level wind shear forecast areas.

References

- Barnes, S. L., 1964: "Techniques for Maximizing Details in Numerical Weather Analysis," Journal of Applied Meteorology, Vol. 3, No. 4, pp. 396-409.
- Cressman, G. P., 1959: "An Operational Objective Analysis System," Monthly Weather Review, Vol. 87, No. 10, pp. 367-374.
- Deeming, J. E., et al., 1972: "National Fire Danger Rating System," USDA Forest Service Research Paper, RM 84.
- Fisher, E. L., and P. Caplan, 1963: "An Experiment in Numerical Prediction of Fog and Stratus," Journal of the Atmospheric Sciences, Vol. 20, No. 5, pp. 425-437.
- Fugita, T. T., et al., 1970: "Palm Sunday Tornadoes of April 11, 1965," Monthly Weather Review, Vol. 98, No. 1, pp. 29-69.
- Gerrity, J. P., 1967: "A Physical-Numerical Model for the Prediction of Synoptic-Scale Low Cloudiness," Monthly Weather Review, Vol. 95, No. 5, pp. 261-282.
- Hadeen, K. D., 1970: "AFGWC Boundary Layer Model," Air Force Global Weather Central Technical Memorandum 70-5, 53 pp.
- Leahey, D. M., 1969: "Mathematical Models of Urban Air Pollution Dynamics - An Urban Heat Island Model," New York University, AP-00328-04.
- Lettau, H. H., 1959: "Wind Profile, Surface Stress, and Geostrophic Drag Coefficients in the Atmospheric Surface Layer," Advances in Geophysics, Vol. 6, Academic Press, New York, pp. 241-257.
- Miller, M. E., and G. Holzworth, 1967: "An Atmospheric Diffusion Model for Metropolitan Areas," J. Air Poll. Control Assoc., 17, pp. 46-50.
- Summers, P. W., 1965: "An Urban Heat Island Model, It's Role in Air Pollution Problems with Application to Montreal." Presented at First Canadian Conference on Micrometeorology, Toronto, 12-14 April, 1965.

List of Figures

- Fig. 1 - Grid lattice of PBL and LFM models.
- Fig. 2 - Vertical depiction of NMC Planetary Boundary Layer model.
- Fig. 3 - Structure of PBL analysis program.
- Fig. 4 - First guess vertical structure in PBL analysis.
- Fig. 5 - Processed sounding - illustrates smoothing effect of interpolated raw data.
- Fig. 6-8 Sounding profile models.
- Fig. 9 - Time cross section.
- Fig. 10 - Schematic of prognostic sounding and teletypewriter message.

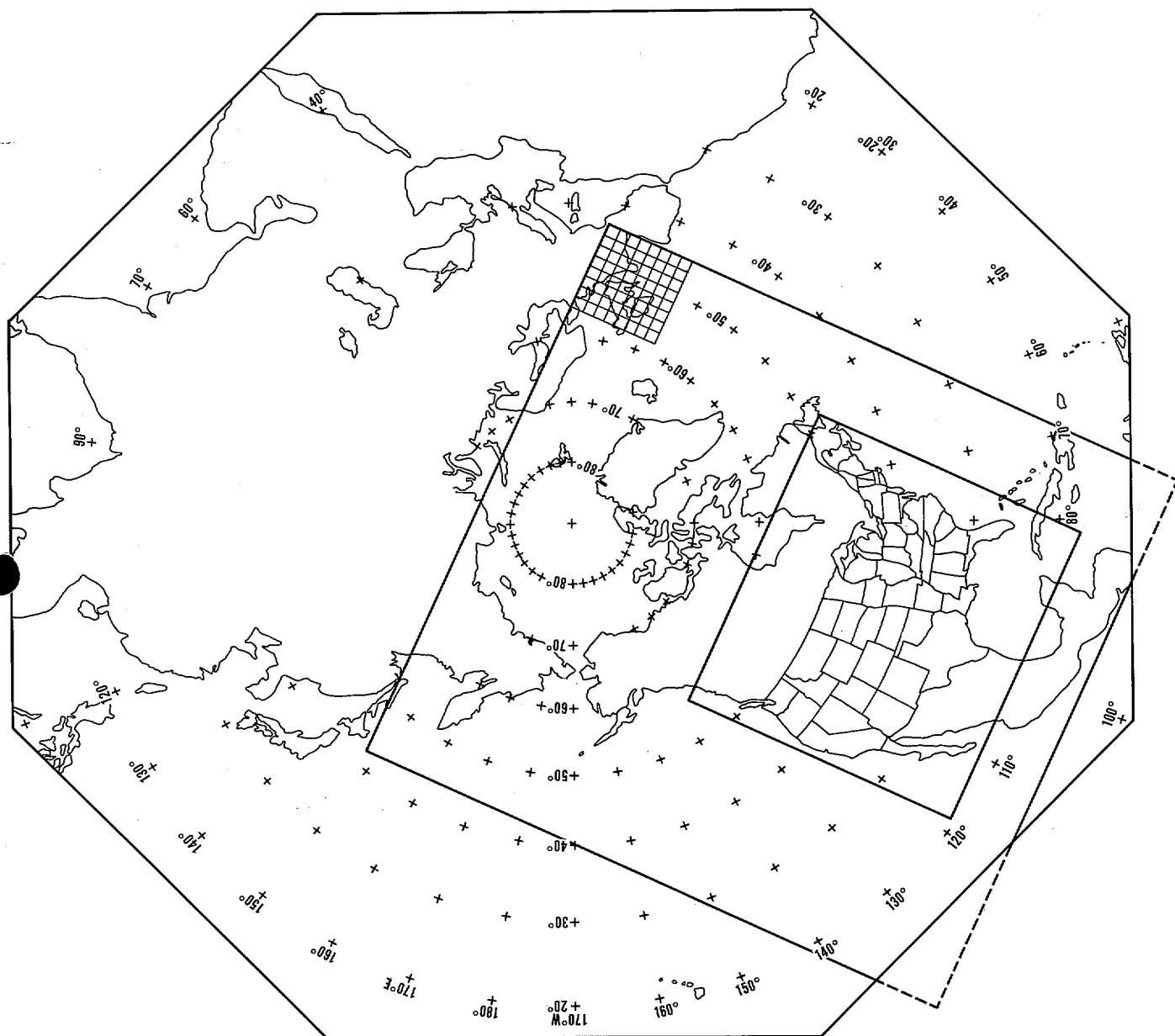
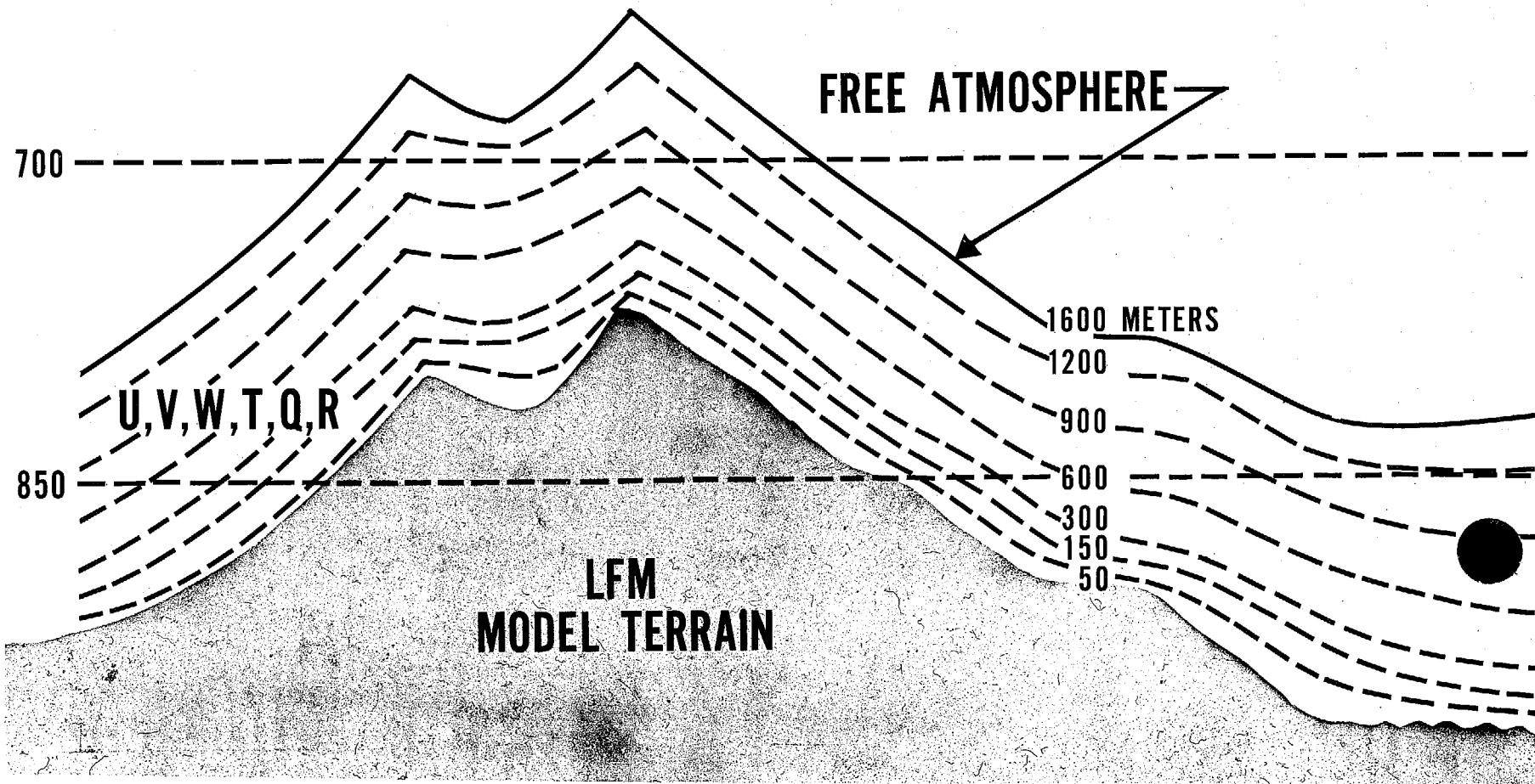


Fig. 1

VERTICAL DEPICTION OF NMC PLANETARY BOUNDARY LAYER MODEL

MB
500 — — — — —

(LFM-U AND V WIND COMPONENTS AND RELATIVE HUMIDITY)



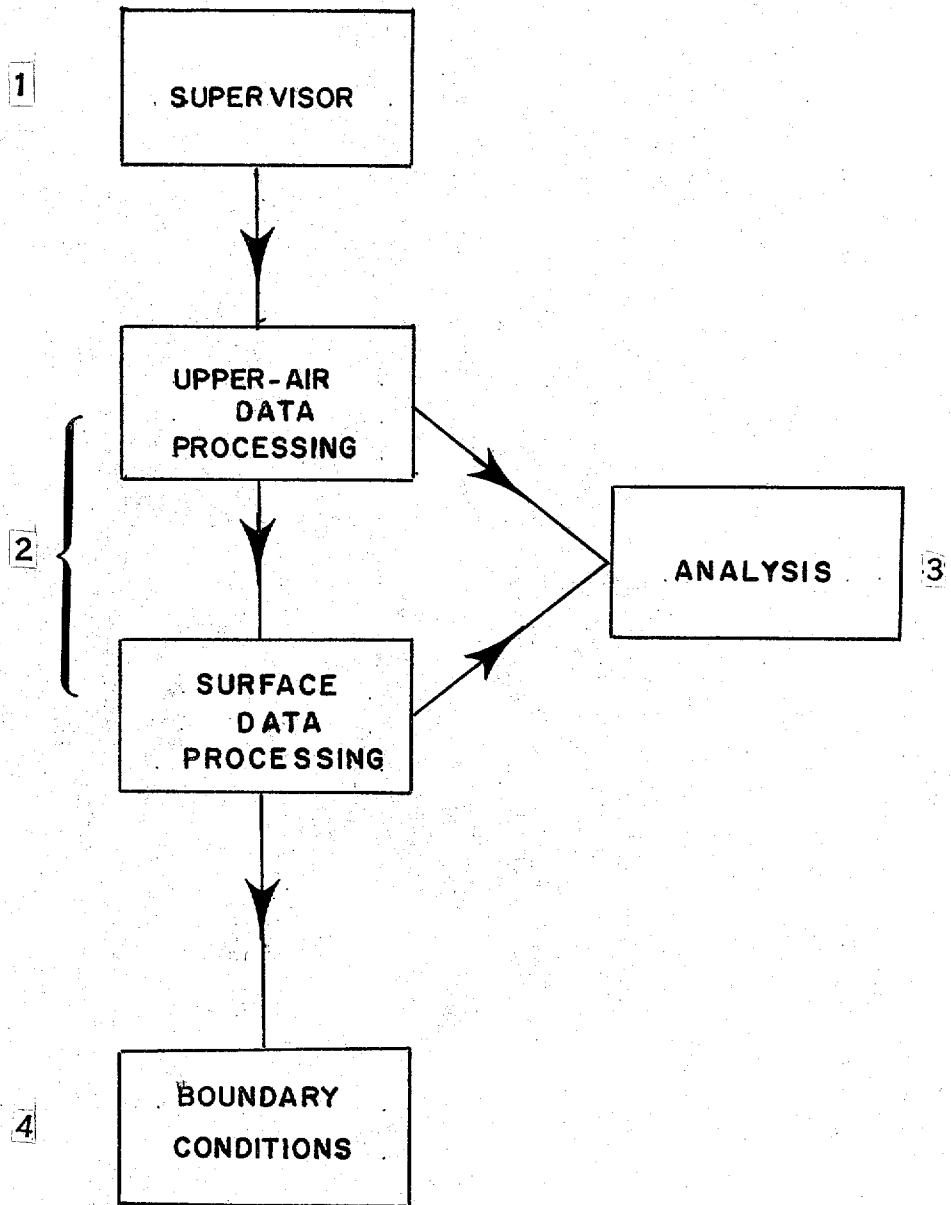


Fig. 3

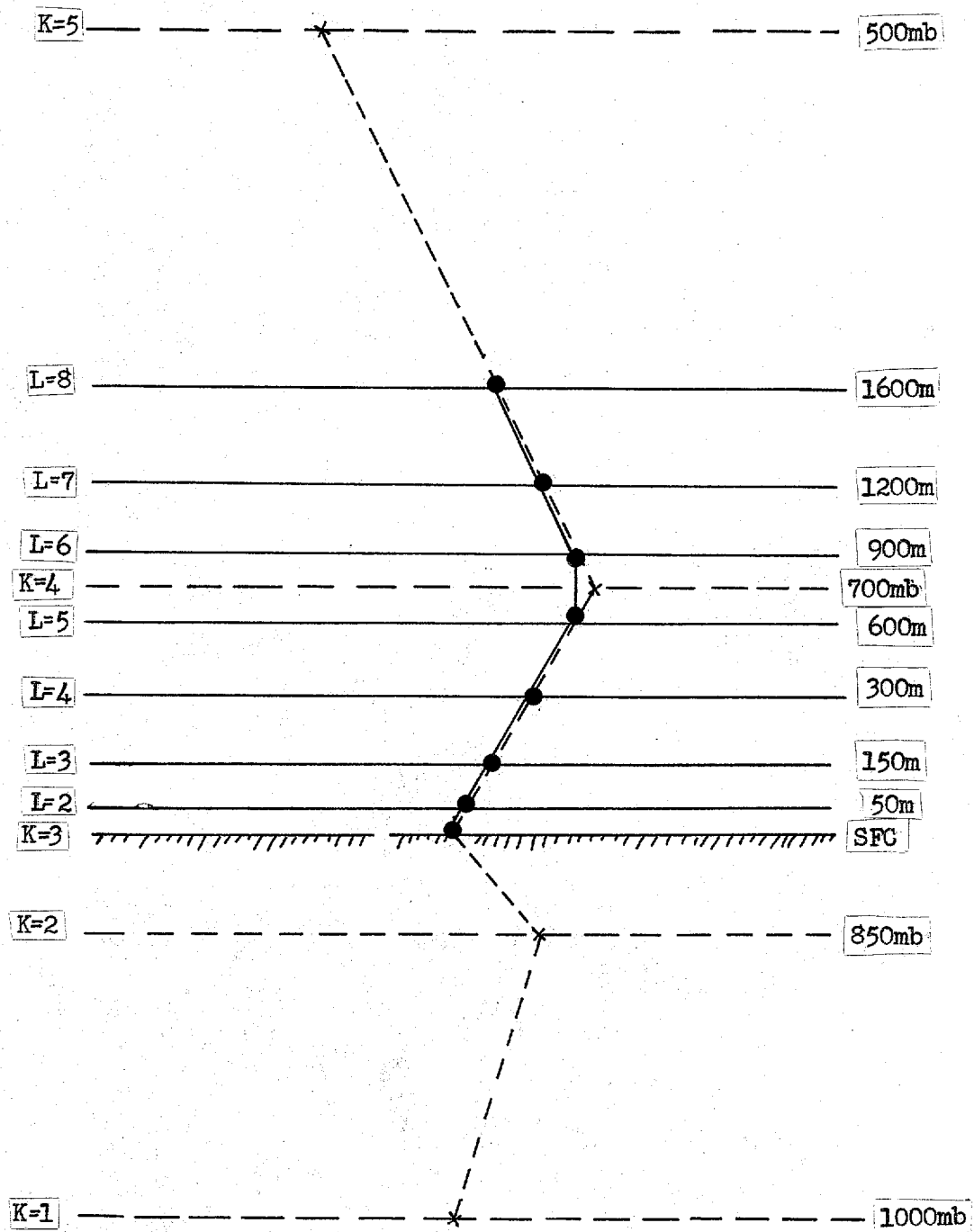
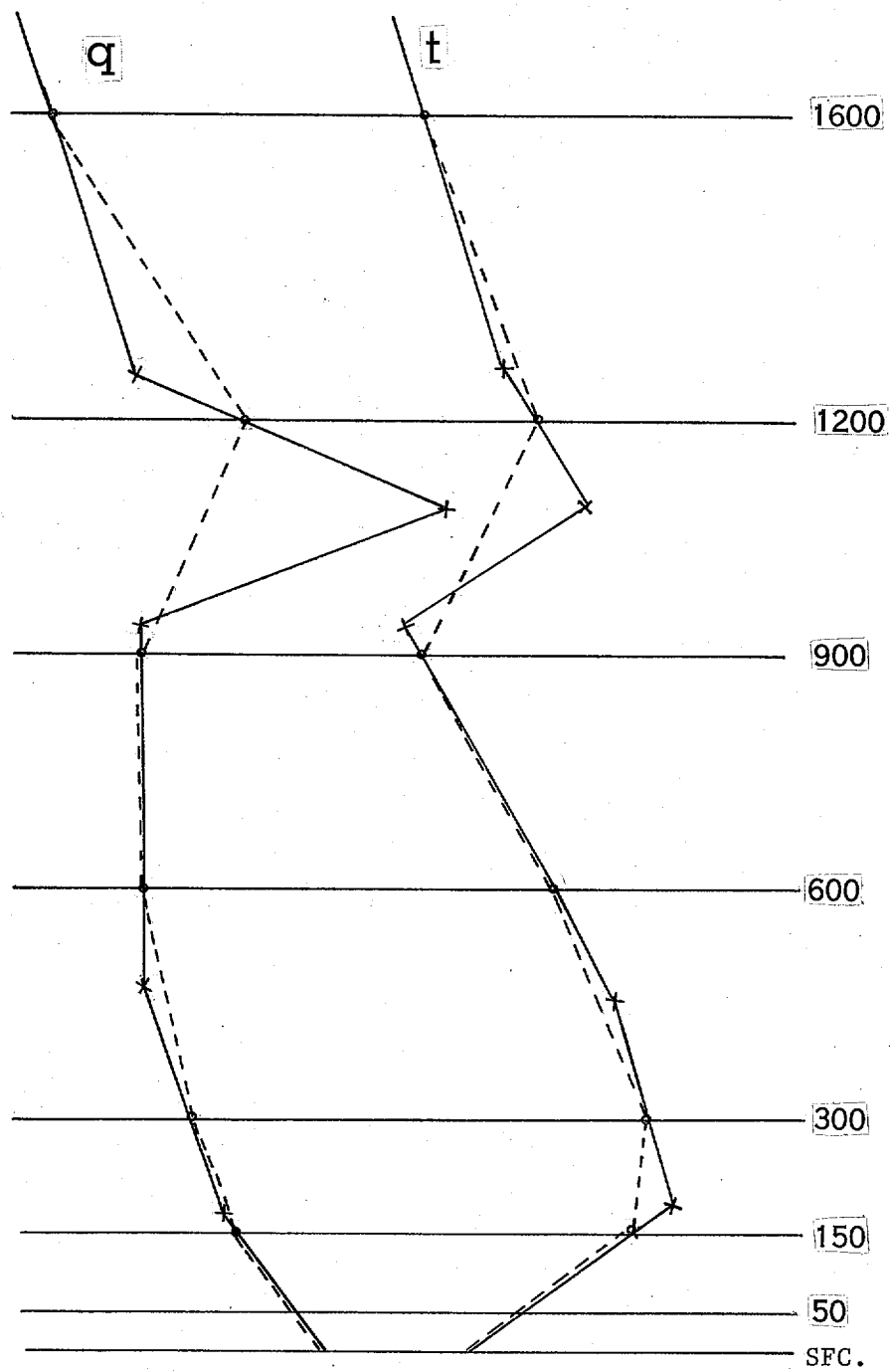


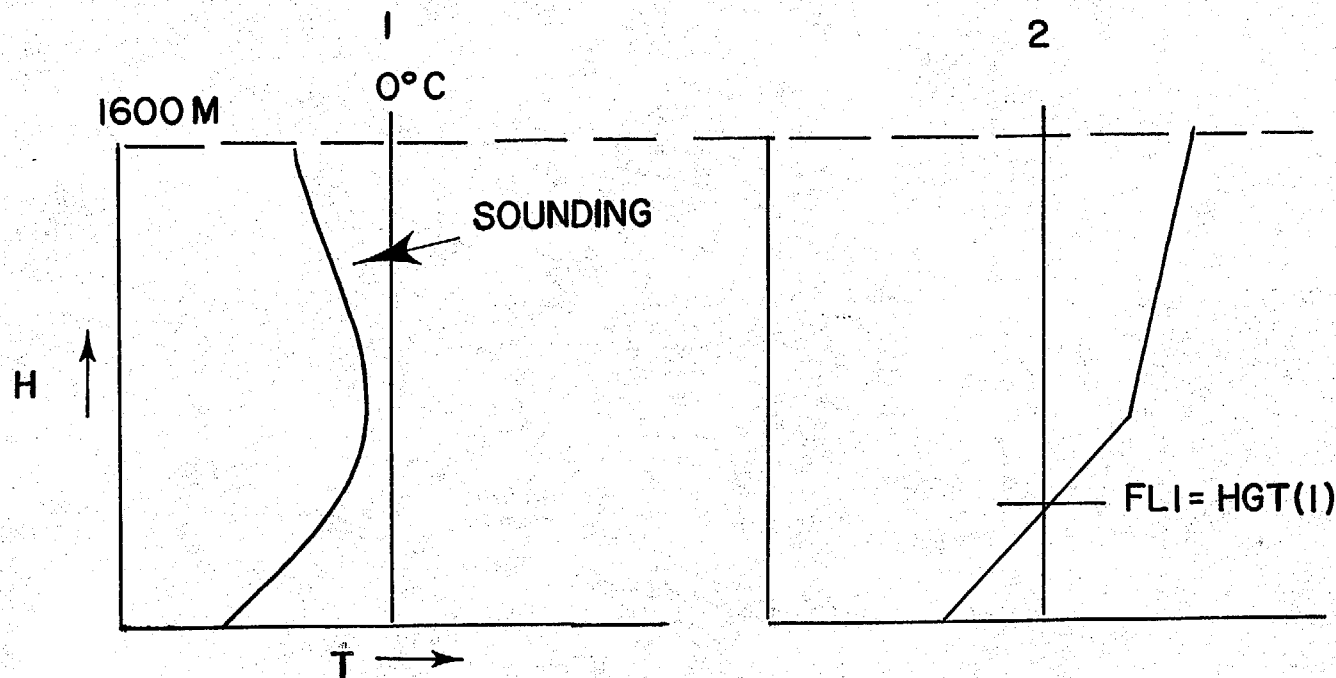
Fig. 4



— OBSERVED
 --- MODEL

Fig. 5 - An example of the model's representation of a typical sounding.

FIG 6



**SOUNDING
CONFIGURATION
USED IN FREEZING
LEVEL ICING
PRECIPITATION TYPE
AND AIR POLLUTION
METEOROLOGY IN
NMC PBL MODEL**

BF = BELOW FREEZING
AF = ABOVE FREEZING
FLI = FIRST FREEZING
LEVEL

FL2 = SECOND FL

R = RAIN

S = SNOW

F = FROZEN

M = MIXED R/S

I = ICING THROUGHOUT
PBL

B = ICING BELOW FL 1

A = ICING ABOVE FL 2

FREEZING
LEVEL

SFC

BF
BF
BF

SFC

AF
FLI
BF

IF MRH > 75 %

IF FLI ≤ 1900 M R/S

PRECIP

S

F

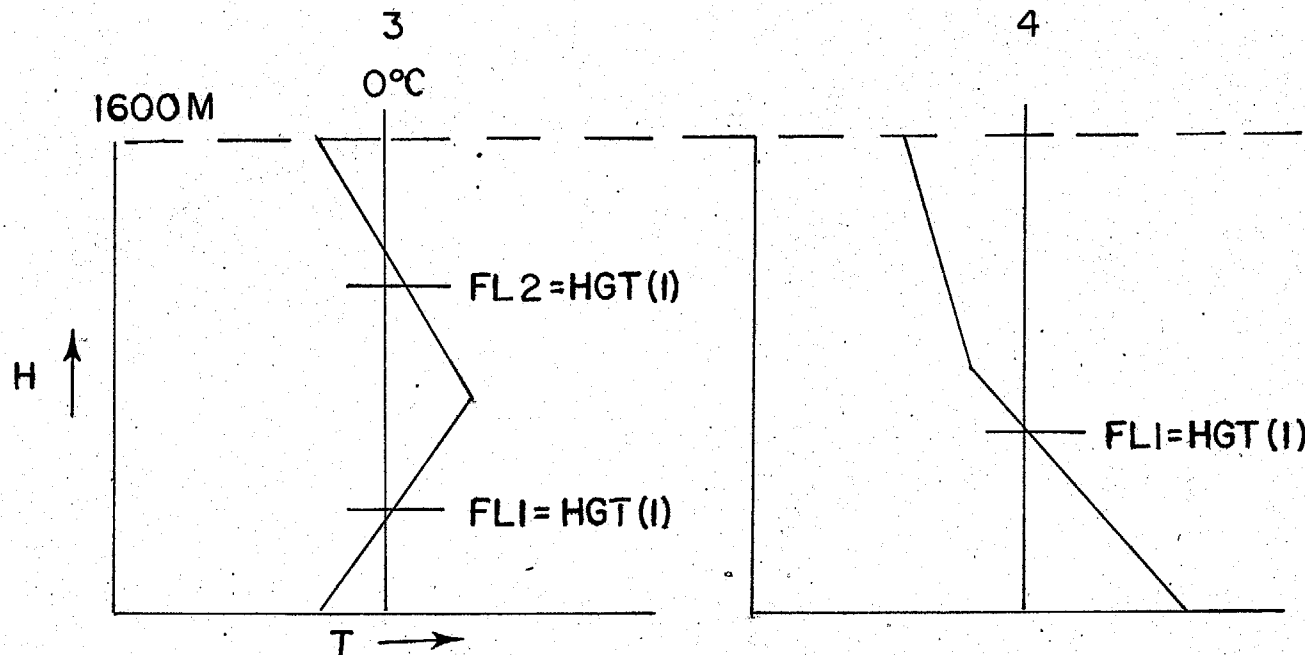
ICING

IF MRH ≥ 75

I

B

FIG 7



**SOUNDING
CONFIGURATION
USED IN FREEZING
LEVEL ICING
PRECIPITATION TYPE
AND AIR POLLUTION
METEOROLOGY IN
NMC PBL MODEL.**

**FREEZING
LEVEL**

SFC **FL2**
FL1
BF

SFC **BF**
FL1
AF

PRECIP

IF FL1 ≤ 900M R/S

IF MRH ≥ 75

IF FL1 ≤ 1900M R/S

F

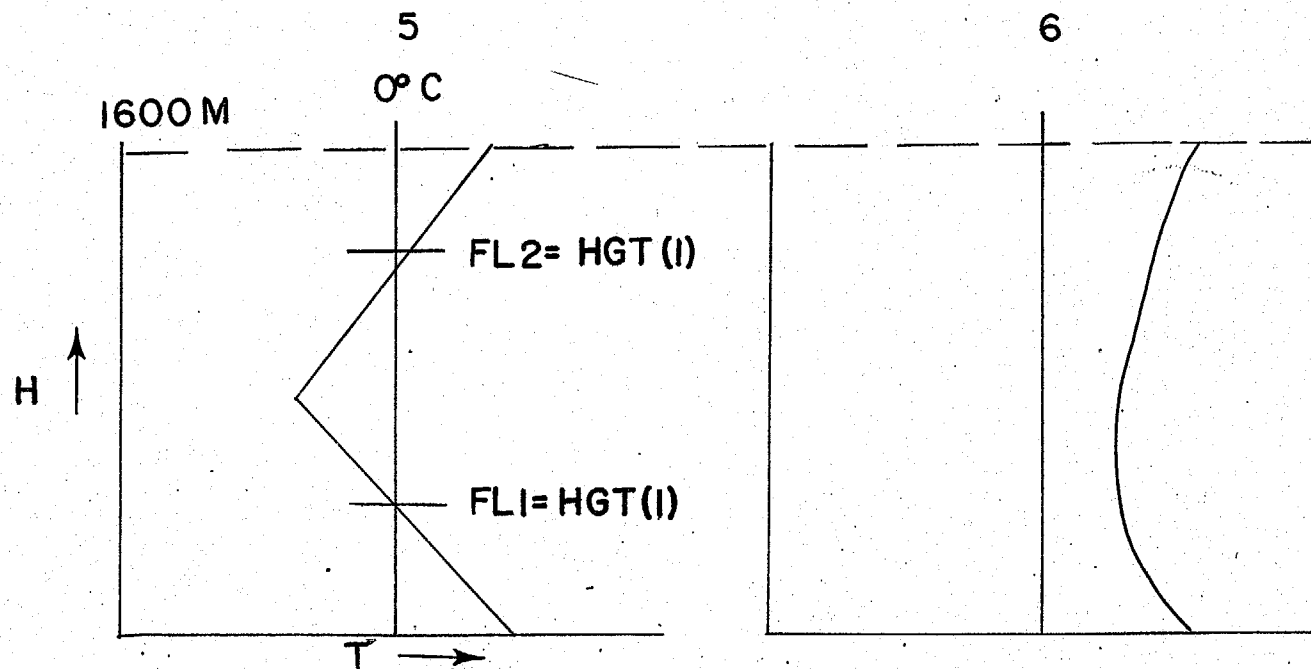
R

ICING

IF MRH ≥ 75 BA

A

FIG 8



**SOUNDING
CONFIGURATION
USED IN FREEZING
LEVEL ICING
PRECIPITATION TYPE
AND AIR POLLUTION
METEOROLOGY IN
NMC PBL MODEL.**

FREEZING		FL 2		AF
LEVEL		FL 1		AF
	SFC	AF	SFC	AF
<hr/>				
	IF FL1 ≤ 1900 R/S			
PRECIP	IF (FL 2 - FL 1)	1900 S		R
<hr/>				
		F		
ICING				
	IF MRH ≥ 75	A		NONE

Fig. 10